International Journal on Interactive Design and Manufacturing (IJIDeM)
https://doi.org/10.1007/s12008-023-01308-6

ORIGINAL PAPER

Optimization of friction stir welding processes using multi-attributive border approximation area comparison (MABAC) method in neutrosophic fuzzy environment

Srinjoy Chatterjee[1] · **Shankar Chakraborty**[1]

Received: 20 January 2023 / Accepted: 17 March 2023
© The Author(s), under exclusive licence to Springer-Verlag France SAS, part of Springer Nature 2023

Abstract

The ability to produce high quality joints, with improved mechanical and metallurgical properties, without any harmful emissions, has caused friction stir welding (FSW) to emerge as an efficient and eco-friendly solid-state welding method that has widespread use in many of the industries, especially railway, aerospace and automotive industries. However, the quality of weld produced by FSW process is significantly impacted by the welding parameters involved. To obtain the optimal values of FSW parameters, multi-criteria decision making (MCDM) methods have proven to be an effective way of dealing with multiple input parameters and conflicting responses. Relative importance assigned to various weld characteristics by the concerned stakeholders (welders, process engineers and end users) also greatly influences the final decision with respect to optimal combination of different input parameters for a given welding operation. In this paper, application of a newly developed MCDM tool, in the form of multi-attributive border approximation area comparison (MABAC) method in neutrosophic fuzzy environment considering truth-membership, indeterminacy-membership and falsity-membership functions in a single decision making framework for parametric optimization of two FSW processes is demonstrated. The optimal combination of input parameters for the first FSW process is obtained as tool rotational speed = 1200 rpm, welding speed = 275 mm/min, shoulder diameter = 18 mm and taper-cylindrical tool pin profile. On the other hand, in the second FSW process, an optimal parametric intermix of tool rotational speed = 1000 rpm, traverse speed = 140 mm/min, tool offset = 1 mm and tilt angle = 1.5° would provide the most desired values of the weld characteristics under consideration. This integrated approach would thus help in effectively optimizing FSW processes in single-valued neutrosophic fuzzy environment.

Keywords FSW process · Optimization: MABAC method · Single-valued neutrosophic set

1 Introduction

The increasing need for stronger and more complex components in every industry, to satisfy their demands for more efficient and light-weight parts/components, cannot be fulfilled by welding of similar materials only. This creates a demand for developing joining processes for dissimilar materials which can produce composite parts/components providing benefits of both the materials. The traditional fusion welding processes of the past are not suitable for welding of dissimilar materials. Therefore, the present-day research has been focused on solid-state welding processes [1]. Friction stir welding (FSW) has emerged out as an energy-efficient and environment-friendly solid-state welding process that can efficiently weld dissimilar materials with varying physical and chemical properties. Compared to the conventional metal inert gas welding (MIG) and tungsten inert gas welding (TIG), FSW process has lower heat input which significantly reduces width of the heat-affected zone (HAZ). The FSW process also has added benefits, like it does not require any filler material or shielding gas, and produces no harmful fumes or ultraviolet rays, making it one of the most promising solid-state metal joining processes [2].

The FSW process was developed and patented by The Welding Institute (TWI) in the United Kingdom in 1991. It is a solid-state joining method that can join similar or dissimilar materials using frictional heat generated at the interface without melting the workpieces. In this process, the workpieces to be joined are held together tightly while a rotating tool moves

✉ Shankar Chakraborty
s_chakraborty00@yahoo.co.in

[1] Production Engineering Department, Jadavpur University, Kolkata, West Bengal, India

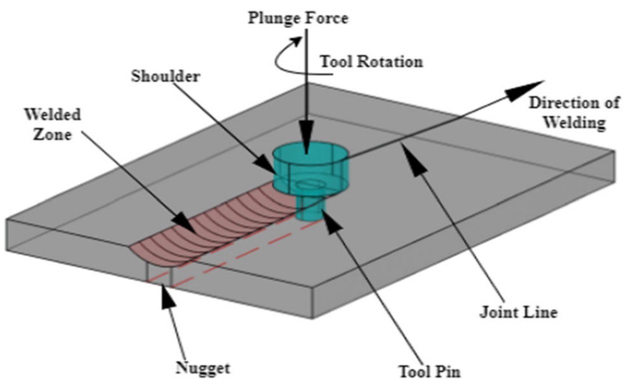

Fig. 1 Schematic representation of an FSW

along the joining line. The tool, with a high rotation rate, is plunged into the workpieces and generates friction at the faying surface. The heat generated due to friction between the tool and the workpiece surfaces leads to intense localized heating that softens the workpiece materials enough to plasticize them without melting. The rotating tool stirs the plasticized materials together by moving them in its direction of rotation. Therefore, the workpieces are joined together by mechanically mixing the two materials through extensive plastic deformation. Since it is a solid-state process, it can avoid defects caused by state changes, such as hot cracking [3, 4]. A schematic representation of FSW process is provided in Fig. 1.

The FSW process has several advantages over the conventional fusion welding techniques, including elimination of cracking due to state change (solidification and liquation), porosity, and enhanced mechanical and metallurgical properties, such as ductility, hardness, fatigue and corrosion resistance. These benefits have led to its widespread use in many of the industries, especially aerospace and automotive industries. The microstructural analysis of joints produced by FSW has verified the enhanced properties of these joints due to grain structure refinement, densification and uniform distribution of alloying elements [5–7]. However, like all other joining processes, the quality of joints produced by FSW is significantly affected by various input parameters. Those process parameters, such as tool rotational speed (TRS), traverse/welding speed (WS), axial/plunge force (AF), plunge depth (PD), tilt angle (TA) etc. must be calibrated to their optimal values to achieve the best weld quality. The tool rotation is responsible for generating frictional heat at the tool-workpiece interface and would melt the material if it is too high or not stir the material properly if it is too low. The welding/traverse speed propagates this heat along the joint line and setting it to a high value would reduce the joint temperature due to uneven distribution of the frictional heat. In addition to these parameters, tool geometry, and shape and size of the shoulder and pin also significantly influence the quality of joints produced [8]. Therefore, it should be noted that the settings of these parameters should neither be too high nor too low as they impact the output parameters, such as ultimate tensile strength (UTS), yield strength (YS), percentage of elongation (PE), hardness, grain size etc. which are considered to determine quality of the welded joint.

Optimization of the process parameters is a challenging task as the impact of multiple input parameters need to be measured with respect to multiple output parameters. To resolve this issue, multi-criteria decision making (MCDM) techniques can act as suitable multi-objective optimization methods to compute the optimal parameter settings. The application of MCDM techniques in fuzzy environment effectively deals with variation in the subjective opinions of different experts with respect to importance associated with each criterion (response/output) involved in optimization of FSW parameters. Depending on varying requirements, the stakeholders (welders/process engineers/end users) involved in FSW process may provide dissimilar importance to different weld characteristics which is often expressed using qualitative terms. They should feel highly relaxed to evaluate the relative importance of the weld features as 'very important', 'moderately important', 'important', 'less important', 'unimportant' and so on. Similarly, it would always be straightforward to assess the measured response values against each of the experiments as 'extremely good', 'good', 'moderately good', 'moderately bad', 'bad', 'extremely bad' and so on. In this paper, a newly developed and well accepted MCDM tool, i.e. multi-attributive border approximation area comparison (MABAC) method is applied in neutrosophic fuzzy (NF) environment while considering truth-membership, indeterminacy-membership and falsity-membership functions in a single decision making framework to determine the optimal parametric settings of two FSW processes using past experimental data. The remaining sections of this paper are structured as follows: A brief literature review of different MCDM techniques in fuzzy environment applied for FSW processes optimization is provided in Sect. 2. Section 3 outlines the mathematical formulation of MABAC method integrated with single-valued neutrosophic sets (SVNS). Section 4 demonstrates the applications of this approach for optimizing two FSW processes and Sect. 5 concludes the paper.

2 Literature review

In this section, a brief review of the literature focussing on the applications of various MCDM techniques to achieve optimal combinations of FSW parameters in fuzzy environment is provided. Table 1 summarizes the reviewed literature while providing information on the work material(s) joined, welding parameters considered for optimization, output responses

Table 1 Optimization of FSW processes in fuzzy environment

Author(s)	Work material(s)	Welding parameters	Response(s)	Method
Shehabeldeen et al. [9]	AA2219-T87	TRS, WS, F	UTS	ANFIS-HHO
Nguyen et al. [10]	AA5052, AA6061	TRS, WS, PD, TA	Energy consumed, UTS, PE	ANFIS, VCPSO-CCS
Van and Nguyen [11]	AA6061	TRS, WS, PD, TA	SWE, JE, MH	Taguchi method, ANFIS, NCGA
Babajanzade Roshan et al. [12]	AA7075	TRS, WS, pin profile, axial Force	UTS, YS, hardness	ANFIS, SA
Vijayan and Seshagiri Rao [13]	AA2024, AA6061	TRS, WS, axial load, pin profile	UTS, TE	RSM, ANFIS
Deepandurai and Parameshwaran [14]	AA7075/SiCp composite plates	TRS, WS, AF, % of reinforcement, tool geometry	UTS, PE	Fuzzy-GRA
Parida and Pal [15]	Aluminium plates	PD, TRS, WS, tool geometry, SD, pin diameter, tool pin length, dwell time	UTS, YS, PE, weld bead thickness, nugget zone hardness	Taguchi method, GRA, fuzzy inference system
Sahu et al. [16]	AA1050 and pure Cu plates	TRS, WS, tool offset, PD	UTS, YS, PE, compressive strength, bending angle, weld bead thickness, average hardness	Taguchi method, GRA, fuzzy inference system

measured and MCDM methodology(s) deployed to derive the optimal parametric settings. From Table 1, it is clear that most of the previous literature concerning optimization of FSW processes in fuzzy environment have involved in employment of adaptive neuro-fuzzy inference system (ANFIS) in conjunction with different optimization techniques [9–13]. Grey relational analysis (GRA) has also been used in multiple studies [14–16].

In the study by Shehabeldeen et al. [9], the authors optimized an FSW process with respect to a single response (UTS), by considering three welding parameters, i.e. TRS, WS and plunge force (F) using ANFIS coupled with Harris hawks optimizer (HHO). Considering TRS, WS, PD and TA as the input parameters, Nguyen et al. [10] endeavoured to determine their optimal values to simultaneously minimize energy consumption, and maximize UTS and PE during FSW process based on ANFIS model coupled with vibration and communication particle swarm optimization (VCPSO) and combined compromise solutions (CCS) approaches. A similar work was also carried out by Van and Nguyen [11] using Taguchi design-based ANFIS models with neighbour cultivation genetic algorithm (NCGA) in which specific welding energy (SWE) was minimized, and joint efficiency (JE) and micro-hardness (MH) were maximized at the optimal settings of TRS, WS, PD and TA. In an early 2013 work, Babanjazade Roshan et al. [12] adopted ANFIS model in combination with simulated annealing (SA) to search out the optimal parametric combination for FSW of AA7075 aluminium alloy. In Vijayan and Seshagiri Rao [13], the authors considered four welding parameters, i.e. TRS, WS, axial load and pin profile, and tested UTS and tensile elongation (TE) values of AA2024 and AA6061 dissimilar welded joints. The performance of a response surface methodology (RSM)-based approach was compared against that of a developed ANFIS model while optimizing the UTS and TE values. It was noticed that the estimates provided by the ANFIS model were better than those obtained based on the RSM model for both the weld characteristics.

Besides ANFIS model, another major methodology that has been explored in the context of fuzzy parametric optimization of FSW processes includes GRA technique. In Deepandurai and Parameshwaran [14], the authors performed multi-response optimization of an FSW process using a fuzzy inference-integrated GRA technique based on RSM model. On the other hand, Parida and Pal [15] and Sahu et al. [16] presented the application of GRA along with fuzzy inference system and Taguchi methodology respectively. Furthermore, an overview of the optimization-related studies conducted for FSW processes can be found in [17, 18]. Based on the survey of the existing literature of parametric optimization of FSW processes, it can be noticed that no research has been conducted till date on the application of any of the MCDM techniques in NF environment to optimize FSW processes. Therefore, to address this potential research gap, this paper proposes integration of MABAC with SVFS to carry out multi-objective optimization of two

FSW processes based on past experimental data. To deal with imprecise information in complex scenarios, fuzzy set theory [19] has already been proved to be an effective tool. However, fuzzy sets are only characterized by membership function and therefore, are unable to deal with non-membership and incompleteness of information. On the other hand, intuitionistic fuzzy sets (IFSs) [20] are characterized by membership and non-membership functions to overcome the drawback of conventional fuzzy sets. But, IFSs are restricted by the level of indeterminacy they can handle as the sum of the membership, non-membership and hesitancy degrees of IFSs should always be equal to one. Neutrosophic set theory, developed by Smarandache in 1999 [21], proposes a generalization of conventional fuzzy sets and IFSs considering truth-membership (T), indeterminacy-membership (I) and falsity-membership (F) independent of each other. This unique property of neutrosophic fuzzy sets (NFSs) allows them to be integrated with different MCDM tools to solve complex decision making problems [22]. To address the research gaps identified through survey of the existing literature, this paper contributes the following:

(a) A neutrosophic fuzzy environment is considered for optimizing the input parameters of two FSW processes which would overcome the shortcomings of the traditional MCDM techniques in standard fuzzy and intuitionistic fuzzy environments. To the best of the authors' knowledge, no prior study has been carried out on parametric optimization of any of the manufacturing processes in neutrosophic fuzzy environment.
(b) A relatively new MCDM approach in the form of MABAC method in combination with SVNS is employed to carry out discrete optimization of FSW process parameters.
(c) Using MABAC method, all the FSW experiments are segregated into upper and lower approximation areas which would help in identifying and analyzing the shortcomings of the underperforming experiments lying in the lower approximation area. The FSW experiments positioned in the upper approximation area can thus be treated as the benchmarks for the underperforming trials.

The procedural steps involved in SVNS-MABAC method for parametric optimization of FSW processes are presented in the form of a flowchart, as shown in Fig. 2.

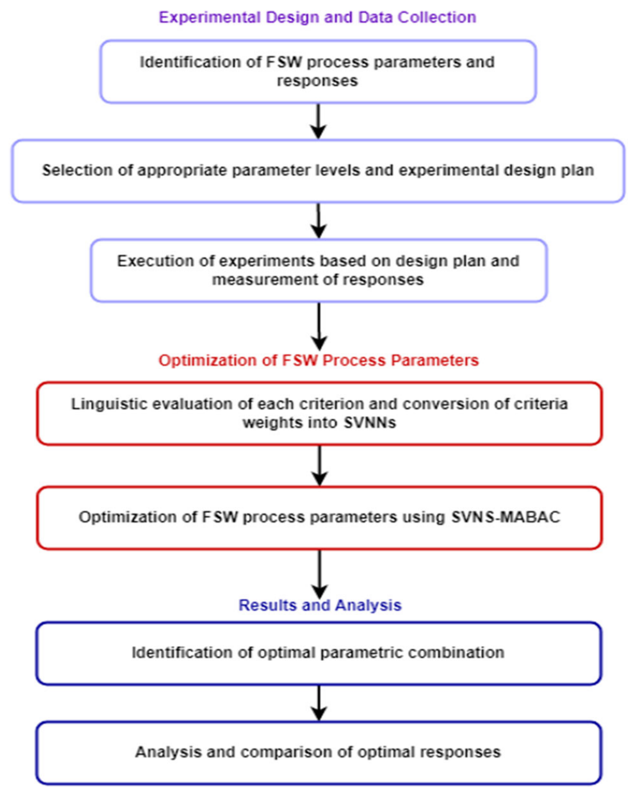

Fig. 2 Flowchart for SVNS-MABAC method-based optimization of FSW processes

3 Methods

3.1 3.1 Neutrosophic sets

Neutrosophic sets were proposed by Smarandache [21] as a derivative of neutrosophy, a branch of philosophy that studies the origin, nature and scope of neutralities, as well as their interactions with different ideational spectra. It is a generalization of classical fuzzy set and IFS theories, based on neutrosophy, to overcome their drawbacks of dealing with indeterminacy. According to Smarandache [21], a neutrosophic set A in a space of points X is defined by a truth-membership function T_A, an indeterminacy-membership functionI_A and a falsity-membership functionF_A. The functions$T_A(x)$, $I_A(x)$ and$F_A(x)$ are real standard or non-standard subsets of$]0^-, 1^+[$. It means that $T_A(x) : X \to \left]0^-, 1^+\right[$, $I_A(x) : X \to \left]0^-, 1^+\right[$ and $F_A(x) : X \to \left]0^-, 1^+\right[$. There is also no restriction on the sum of $T_A(x)$, $I_A(x)$ and$F_A(x)$, so $0^- \le supT_A(x) + supI_A(x) + supF_A(x) \le 3^+$.

3.2 Single-valued neutrosophic sets

The SVNSs, proposed by Wang et al. [23], are a special instance of neutrosophic sets which can be applied to model real-world scientific and engineering problems. A SVNS A in a space of points X can be defined as below:

$$A = \{\langle x, T_A(x), I_A(x), F_A(x)\rangle | x \in X\} \tag{1}$$

Here, $T_A(x), I_A(x), F_A(x) \in [0,1]$ for all x in X, and denote the truth-membership, indeterminacy-membership and falsity-membership functions respectively.

For two SVNSs A and B, the basic arithmetic operations can be defined as follows:

$$A \oplus B = \{\langle T_A(x) + T_B(x) - T_A(x) \cdot T_B(x), I_A(x) \cdot I_B(x), \times\ F_A(x) \cdot F_B(x) | x \in X\} \tag{2}$$

$$A \otimes B = \{\langle T_A(x) \cdot T_B(x), I_A(x) + I_B(x) - I_A(x) \cdot I_B(x), F_A(x) + F_B(x) - F_A(x) \cdot F_B(x)\rangle | x \in X\} \tag{3}$$

$$\lambda A = \left\{\left\langle 1 - (1 - T_A(x))^{\lambda}, I_A(x)^{\lambda}, F_A(x)^{\lambda} | \right\rangle x \in X\right\} \tag{4}$$

$$A^{\lambda} = \left\{\left\langle T_A(x)^{\lambda}, 1 - (1 - I_A(x))^{\lambda}, 1 - (1 - F_A(x))^{\lambda} | \right\rangle x \in X\right\} \tag{5}$$

The score function (S) is considered to convert a single-valued neutrosophic number (SVNN) into a real number, which can be defined as below:

$$S(A) = \frac{3 + T_A(x) - 2I_A(x) - F_A(x)}{4} \tag{6}$$

If the score of SVNS A is less than that of SVNS B, SVNS A is considered to be lesser than SVNS B. The Euclidean distance between two SVNSs A and B, having n elements in each, is defined as:

$$D_{Eu}(A, B) = \sqrt{\sum_{i=1}^{n}\left\{(T_A(x_i) - T_B(x_i))^2 + (I_A(x_i) - I_B(x_i))^2 + (F_A(x_i) - F_B(x_i))^2\right\}} \tag{7}$$

The normalized Euclidean distance is provided in the following equation:

$$D_{Eu}^{N}(A, B) = \sqrt{\frac{1}{3n}\sum_{i=1}^{n}\left\{(T_A(x_i) - T_B(x_i))^2 + (I_A(x_i) - I_B(x_i))^2 + (F_A(x_i) - F_B(x_i))^2\right\}} \tag{8}$$

In most of the decision making problems, it is quite common to have multiple decision makers evaluating the relative importance of the criteria considered and performance of the alternatives with respect to each criterion. Thus, it is necessary to aggregate their evaluations into a single framework (matrix), considering weights assigned to each decision maker, in order to proceed with further calculations. While considering application of any of the MCDM methods in single-valued neutrosophic environment, single-valued neutrosophic weighted averaging (SVNWA) operator allows to aggregate the opinions of multiple decision makers. Let us consider that an MCDM problem involves l decision makers, and $\tilde{w}_j^{(k)} = \left[T_j^{(k)}, I_j^{(k)}, F_j^{(k)}\right]$ denotes the weight assigned to jth criterion by kth decision maker, in terms of a SVNN. The aggregated criteria weights can now be computed using SVNWA operator as follows:

$$\begin{aligned}\tilde{w}_j &= SVNWA\left(\tilde{w}_j^{(1)}, \tilde{w}_j^{(2)}, \ldots, \tilde{w}_j^{(l)}\right)\\ &= \oplus_{i=1}^{l}\left(\lambda_i \tilde{w}_j^{(i)}\right)\\ &= \left(1 - \prod_{i=1}^{l}(1 - T_j)^{\lambda_i}, \prod_{i=1}^{l} I_j^{\lambda_i}, \prod_{i=1}^{l} F_j^{\lambda_i}\right)\end{aligned} \tag{9}$$

Here, λ_i is the weight of ith decision maker. Similarly, the SVNWA operator can also be adopted to aggregate evaluations of the alternatives against each criterion provided by l decision makers into a single decision matrix.

3.3 SVNS-based MABAC approach

The MABAC method, proposed by Pamučar and Ćirović [24], is based on the distance of criterion rating of each alternative from the border approximation. Let us consider an MCDM problem with alternatives $A = [A_1, A_2, \ldots, A_m]$ and criteria $C = [C_1, C_2, \ldots, C_n]$. The mathematical steps involved in SVNS-based MABAC approach [25] are defined as below:

Step 1 Obtain the weight of each criterion and performance of each alternative with respect to the criteria under consideration in linguistic terms.

Table 2 Experimental data [26]

Exp. No	TRS (rpm)	WS (mm/min)	SD (mm)	TP	UTS (N/mm^2)	YS (N/mm^2)	PE (%)	MH (VH)
1	1050	250	12	1	250.59	204.40	2.42	81.78
2	1050	275	14	1	241.49	196.10	2.13	82.45
3	1050	300	16	2	203.18	167.43	3.41	84.34
4	1050	325	18	2	220.23	168.29	2.76	87.98
5	1125	250	14	2	230.13	181.30	2.45	88.45
6	1125	275	12	2	194.59	151.80	2.04	90.00
7	1125	300	18	1	230.02	182.10	3.10	87.23
8	1125	325	16	1	202.79	159.29	2.93	86.31
9	1200	250	16	1	246.43	194.49	3.86	91.30
10	1200	275	18	1	252.32	190.41	4.68	90.72
11	1200	300	12	2	242.07	201.65	2.96	84.39
12	1200	325	14	2	218.78	175.90	2.43	88.61
13	1275	250	18	2	202.58	154.07	2.70	87.51
14	1275	275	16	2	220.70	150.89	2.34	88.43
15	1275	300	14	1	231.00	176.23	3.10	83.67
16	1275	325	12	1	239.90	169.98	2.76	85.50

Step 2 Compute criteria weights as SVNNs from their linguistic evaluation.

$$\tilde{w} = \left[\widetilde{w_1}, \widetilde{w_2}, \ldots, \widetilde{w_j}, \ldots, \widetilde{w_n}\right] \tag{10}$$

where $\widetilde{w_j} = \langle T_j, I_j, F_j \rangle$ is a SVNN.

Step 3 Form the initial decision matrix in SVN terms by transforming the linguistic evaluation matrix into its corresponding SVNNs.

$$\tilde{N} = [\tilde{n}_{ij}]_{m\times n} \tag{11}$$

where $\tilde{n}_{ij} = T_{ij}, I_{ij}, F_{ij}$ is an SVNN.

Step 4 Formulate the weighted SVN-decision matrix by multiplying the alternative's performance ratings with the corresponding criteria weights.

$$\tilde{N}' = \left[n'_{ij}\right]_{m\times n} \tag{12}$$

where $n'_{ij} = \widetilde{w_j} \otimes \tilde{n}_{ij} = \left\langle T'_{ij}, I'_{ij}, F'_{ij} \right\rangle$.

Step 5 Develop the border approximate area matrix as follows:

$$\tilde{G} = [\tilde{g}_j]_{1\times n};\ \tilde{g}_j = \prod_{i=1}^{m} \left(n'_{ij}\right)^{\frac{1}{m}} = \left\langle \prod_{i=1}^{m} T'^{\frac{1}{m}}_{ij}, 1 - \prod_{i=1}^{m}\left(1 - I'_{ij}\right)^{\frac{1}{m}}, 1 - \prod_{i=1}^{m}\left(1 - F'_{ij}\right)^{\frac{1}{m}} \right\rangle \tag{13}$$

Step 6 Formulate the distance matrix by calculating the Euclidean distance of each element of the weighted SVN-decision matrix from the corresponding element of the border approximate area matrix.

$$D = [d_{ij}]_{m\times n} \text{where,} \tag{14}$$

$$d_{ij} = \begin{cases} D^N_{Eu}(\tilde{n}_{ij}, \tilde{g}_j),\ if \tilde{n}_{ij} > \tilde{g}_j \\ 0,\ if \tilde{n}_{ij} = \tilde{g}_j \\ -D^N_{Eu}(\tilde{n}_{ij}, \tilde{g}_j),\ if \tilde{n}_{ij} < \tilde{g}_j \end{cases}$$

The d_{ij} values signify the location of the alternatives in one of three regions: upper approximation area (G^+), border approximation area (G) and lower approximation area (G^-). The ideal alternative is located in G^+, while the position of a non-ideal alternative is in G^-.

Step 7 Compute the final score of each alternative as the row-wise sum of the distance matrix.

$$Q_i = \sum_{j=1}^{n} d_{ij} \tag{15}$$

Higher Q_i value indicates that the corresponding alternative is closer to the ideal solution. Therefore, the alternatives are ranked in decreasing order of Q_i, with the best alternative having the highest Q_i.

Table 3 Converting responses into linguistic variables for example 1

Linguistic variable	UTS	YS	PE	MH
Extremely good (EG)	UTS ≥ 245.906	YS ≥ 198.454	PE ≥ 4.387	MV ≥ 90.242
Very good (VG)	239.492 ≤ UTS < 245.906	192.508 ≤ YS < 198.454	4.094 ≤ PE < 4.387	89.184 ≤ MH < 90.242
Good (G)	233.078 ≤ UTS < 239.492	186.562 ≤ YS < 192.508	3.801 ≤ PE < 4.094	88.126 ≤ MH < 89.184
Medium good (MG)	226.664 ≤ UTS < 233.078	180.616 ≤ YS < 186.562	3.508 ≤ PE < 3.801	87.068 ≤ MH < 88.126
Medium (M)	220.25 ≤ UTS < 226.664	174.67 ≤ YS < 180.616	3.215 ≤ PE < 3.508	86.01 ≤ MH < 87.068
Medium bad (MB)	213.836 ≤ UTS < 220.25	168.724 ≤ YS < 174.67	2.922 ≤ PE < 3.215	84.952 ≤ MH < 86.01
Bad (B)	207.422 ≤ UTS < 213.836	162.778 ≤ YS < 168.724	2.629 ≤ PE < 2.922	83.894 ≤ MH < 84.952
Very bad (VB)	201.008 ≤ UTS < 207.422	156.832 ≤ YS < 162.778	2.336 ≤ PE < 2.629	82.836 ≤ MH < 83.894
Extremely bad (EB)	UTS < 201.008	YS < 156.832	PE < 2.336	MH < 82.836

Table 4 SVNNs for linguistic evaluation of alternatives [27]

Linguistic variable	T	I	F
EG	1.00	0.00	0.00
VG	0.90	0.10	0.05
G	0.80	0.20	0.15
MG	0.65	0.35	0.30
M	0.50	0.50	0.45
MB	0.35	0.65	0.60
B	0.20	0.75	0.80
VB	0.10	0.85	0.90
EB	0.05	0.90	0.95

Table 5 SVNNs for linguistic evaluation of criteria [27]

Linguistic variable	T	I	F
Very important (VI)	0.90	0.10	0.10
Important (I)	0.80	0.20	0.15
Medium (M)	0.50	0.40	0.45
Unimportant (UI)	0.35	0.60	0.70
Very unimportant (VUI)	0.10	0.80	0.90

4 Optimization of FSW processes

To demonstrate the performance of SVNS-based MABAC approach in solving parametric optimization problems of FSW processes, two illustrative examples using the past experimental data are considered in this paper.

4.1 Example 1

In the first example, the experimental data of Jain and Kumar [26] is taken into account to solve the multi-objective parametric optimization problem of an FSW process. Based on Taguchi's L_{16} orthogonal array design plan, 16 experimental runs were carried out on Al 6061-T6 alloy workpieces with four welding parameters, i.e. TRS, WS, SD and tool pin profile (TP), and four responses, i.e. UTS, YS, PE, and MH. The Al 6061-T6 alloy workpieces, with 150 mm × 100 mm dimensions, were butt-jointed using an FSW process on a conventional vertical milling machine with appropriate fixtures using a non-consumable H13 steel tool. The thickness of the workpieces used was 6 mm. During the FSW process, each input parameter was set to different levels, like TRS (1050, 1125, 1200, 1275 rpm), WS (250, 275, 300, 325 mm/min), SD (12, 14, 16, 18 mm) and TP (1—taper cylindrical, 2—square). The specimens for tensile testing were carefully prepared according to the guidelines set by the American Society for Testing and Materials E8, and tested using a Universal Testing Machine (FIE Pvt. Ltd., India; Model: UTE-40; Maximum capacity: 400 kN) to measure the corresponding UTS, YS and PE values. The MH values were measured through a Vickers micro-hardness test applying an indentation load of 250 gf for a dwell time of 10 s. During Vickers micro-hardness test, the hardness profile was measured at the middle cross-section of the welded samples. The optimal parametric combination for the said process was derived while ranking the experimental runs based on their computed grey relational grades using GRA technique. The experimental data along with different values of welding parameters and responses for each experimental run is provided in Table 2.

During the FSW operation on Al 6061-T6 alloy workpieces, the response variables (UTS, YS, PE and MH) may have varying importance with respect to the impact that they have on the quality of joints produced. Therefore, relative importance is assigned to each of the responses in terms of linguistic variables. The linguistic evaluation of the values obtained for each response in each experimental run is carried out considering nine different linguistic scales depending on the conditions, as provided in Table 3. The linguistic variables are subsequently converted into their corresponding

SVNNs based on the values, as shown in Table 4. For assigning relative importance to individual response, five linguistic variables are considered, as exhibited in Table 5.

For solving this multi-objective parametric optimization problem of the FSW process, the opinion of a single decision maker is considered, based on which the relative importance of UTS is assigned as very important (VI), that of YS and TE as important (I), and of MH as medium (M). Based on these evaluations, the corresponding weights for UTS, YS, PE and MH in terms of SVNNs are obtained as ⟨0.9, 0.1, 0.1⟩, ⟨0.8, 0.2, 0.15⟩, ⟨0.8, 0.2, 0.15⟩ and ⟨0.5, 0.4, 0.45⟩ respectively. Using the values as provided in Tables 3 and 4, the initial SVN-decision matrix is formed, as shown in Table 6. Next, the criteria weights (as SVNNs) are multiplied with the elements of the initial SVN-decision matrix to form the weighted SVN-decision matrix, as depicted in Table 7. The border approximation area matrix, in Table 8, is developed from the values provided in Table 7 using Eq. (13). Finally, the distance matrix is formulated by calculating the Euclidean distance of the elements of the weighted SVN-decision matrix from the corresponding elements of the border approximation area matrix, using Eq. (14). The final score of each experimental run is computed using Eq. (15), as shown in Table 9. The experimental runs are ranked in descending order of the final score. From Table 9, it can be observed that experimental run 10, having welding parameters TRS = 1200 rpm, WS = 275 mm/min, SD = 18 mm and TP = 1 (taper cylindrical) provides the optimal combination of parameters producing a weld joint with UTS = 252.32 N/mm^2, YS = 190.41 N/mm^2, PE = 4.68% and MH = 90.72 VH. Furthermore, run 9 provides the second-best parametric combination while run 6 has the worst parametric intermix. When all the criterion function values (Q_i) for the conducted FSW operations are plotted in Fig. 3, it can be observed that ten experiments are positioned in the upper approximation area, whereas, the locations of the remaining six experiments are in the lower approximation area. The location of experiment number 10 in the extreme left corner of upper approximation area confirms it as the best trial. On the other hand, trial number 6 is positioned in the extreme right corner of lower approximation area identifying it as the worst experiment. Thus, experiments in the upper approximation area are superior in performance as compared to those in the lower approximation area with respect to achieved weld characteristics, and can be treated as the benchmarks to the underperforming experiments. Interestingly, Jain and Kumar [26] obtained the same intermix of the FSW parameters while solving this problem using GRA technique. It proves the applicability and solution accuracy of SVNS-MABAC method in solving parametric optimization problems for FSW processes.

4.2 Example 2

Based on central composite design plan of RSM technique, 30 experimental runs were conducted by Tamjidy et al. [28] to test the mechanical properties of FSW butt-welded AA6061-T6 and AA7075-T6 Al alloys. The dataset of Tamjidy et al. [28] is considered in this paper as the second example to validate the effectiveness of SVNS-MABAC approach as a viable multi-objective optimization tool to solve parametric optimization problem of the FSW process. During FSW experiments, TRS, WS, tool offset (TO) and TA were treated as the input parameters, while UTS, PE and MH were considered as the responses to represent the weld quality. Based on the literature survey, Tamjidy et al. [28] included those input parameters because of their significant influences on the mechanical properties of dissimilar FSW welded joints. The workpieces, with dimensions 100 × 50 × 6 mm, were butt-jointed using an AISI H13 hot work steel tool having a square pin profile. The experiments were conducted by setting the values of four input parameters to five different levels, coded as − 2, − 1, 0, + 1 and + 2, as shown in Table 10. During experiments, tool offset was considered as positive to the right of the center of the test weld specimen and negative to the left. During the FSW operation, AA6061-T6 workpiece was placed on the advancing side where tool traverse had been in the direction of spindle rotation, while AA7075-T6 workpiece was placed on the retreating side. For measuring UTS and PE values, tensile testing was carried out using a precise Universal Testing Machine (Instron 3382) and to measure the MH values, microhardness measurements were taken using a load of 200 g for a dwell period of 20 s. To minimize errors during measuring the corresponding response values, three test specimens were extracted during each experimental run and their average response values were reported. The Pareto optimal frontier was later computed using a multi-objective biogeography-based optimization algorithm, and the optimal combinations of welding parameters, in the afore-mentioned Pareto frontier, were obtained using TOPSIS and Shannon's entropy methods. The experimental results are provided in Table 11.

As mentioned earlier, during FSW operation on dissimilar aluminium alloys, the response variables (UTS, PE and MH) may have varying importance with respect to their impact on the quality of the weld joint produced. The values of the measured responses and each response variable itself are assigned relative importance in linguistic terms, and these linguistic evaluations are subsequently converted into corresponding SVNNs using Tables 4 and 5, as demonstrated in the previous example. Table 12 provides the conditions for converting the responses of each experimental run into linguistic terms.

Likewise the previous example, for solving this parametric optimization problem employing SVNS-MABAC method, the opinion of a single decision maker is also considered,

Table 6 Initial SVN-decision matrix for example 1

Exp. No	UTS			YS			PE			MH		
	T	I	F	T	I	F	T	I	F	T	I	F
E_1	1.00	0.00	0.00	1.00	0.00	0.00	0.10	0.85	0.90	0.05	0.90	0.95
E_2	0.90	0.10	0.05	0.90	0.10	0.05	0.05	0.90	0.95	0.05	0.90	0.95
E_3	0.10	0.85	0.90	0.20	0.75	0.80	0.50	0.50	0.45	0.20	0.75	0.80
E_4	0.35	0.65	0.60	0.20	0.75	0.80	0.20	0.75	0.80	0.65	0.35	0.30
E_5	0.65	0.35	0.30	0.65	0.35	0.30	0.10	0.85	0.90	0.80	0.20	0.15
E_6	0.05	0.90	0.95	0.05	0.90	0.95	0.05	0.90	0.95	0.90	0.10	0.05
E_7	0.65	0.35	0.30	0.65	0.35	0.30	0.35	0.65	0.60	0.65	0.35	0.30
E_8	0.10	0.85	0.90	0.10	0.85	0.90	0.35	0.65	0.60	0.50	0.50	0.45
E_9	1.00	0.00	0.00	0.90	0.10	0.05	0.80	0.20	0.15	1.00	0.00	0.00
E_{10}	1.00	0.00	0.00	0.80	0.20	0.15	1.00	0.00	0.00	1.00	0.00	0.00
E_{11}	0.90	0.10	0.05	1.00	0.00	0.00	0.35	0.65	0.60	0.20	0.75	0.80
E_{12}	0.35	0.65	0.60	0.50	0.50	0.45	0.10	0.85	0.90	0.80	0.20	0.15
E_{13}	0.10	0.85	0.90	0.05	0.90	0.95	0.20	0.75	0.80	0.65	0.35	0.30
E_{14}	0.50	0.50	0.45	0.05	0.90	0.95	0.10	0.85	0.90	0.80	0.20	0.15
E_{15}	0.65	0.35	0.30	0.50	0.50	0.45	0.35	0.65	0.60	0.10	0.85	0.90
E_{16}	0.90	0.10	0.05	0.35	0.65	0.60	0.20	0.75	0.80	0.35	0.65	0.60

Table 7 Weighted SVN-decision matrix for example 1

Exp. No	UTS			YS			PE			MH		
	T	I	F	T	I	F	T	I	F	T	I	F
E_1	0.900	0.100	0.100	0.800	0.200	0.150	0.080	0.880	0.915	0.025	0.940	0.973
E_2	0.810	0.190	0.145	0.720	0.280	0.193	0.040	0.920	0.958	0.025	0.940	0.973
E_3	0.090	0.865	0.910	0.160	0.800	0.830	0.400	0.600	0.533	0.100	0.850	0.890
E_4	0.315	0.685	0.640	0.160	0.800	0.830	0.160	0.800	0.830	0.325	0.610	0.615
E_5	0.585	0.415	0.370	0.520	0.480	0.405	0.080	0.880	0.915	0.400	0.520	0.533
E_6	0.045	0.910	0.955	0.040	0.920	0.958	0.040	0.920	0.958	0.450	0.460	0.478
E_7	0.585	0.415	0.370	0.520	0.480	0.405	0.280	0.720	0.660	0.325	0.610	0.615
E_8	0.090	0.865	0.910	0.080	0.880	0.915	0.280	0.720	0.660	0.250	0.700	0.698
E_9	0.900	0.100	0.100	0.720	0.280	0.193	0.640	0.360	0.278	0.500	0.400	0.450
E_{10}	0.900	0.100	0.100	0.640	0.360	0.278	0.800	0.200	0.150	0.500	0.400	0.450
E_{11}	0.810	0.190	0.145	0.800	0.200	0.150	0.280	0.720	0.660	0.100	0.850	0.890
E_{12}	0.315	0.685	0.640	0.400	0.600	0.533	0.080	0.880	0.915	0.400	0.520	0.533
E_{13}	0.090	0.865	0.910	0.040	0.920	0.958	0.160	0.800	0.830	0.325	0.610	0.615
E_{14}	0.450	0.550	0.505	0.040	0.920	0.958	0.080	0.880	0.915	0.400	0.520	0.533
E_{15}	0.585	0.415	0.370	0.400	0.600	0.533	0.280	0.720	0.660	0.050	0.910	0.945
E_{16}	0.810	0.190	0.145	0.280	0.720	0.660	0.160	0.800	0.830	0.175	0.790	0.780

Table 8 Border approximation area matrix for example 1

Criteria	UTS			YS			PE			MH		
	T	I	F	T	I	F	T	I	F	T	I	F
G	0.368	0.585	0.614	0.256	0.693	0.717	0.166	0.791	0.816	0.192	0.735	0.780

Table 9 Results of the SVNS-MABAC-based optimization for example 1

Exp. No	UTS	YS	PE	HH	Q_i	Rank
E_1	0.885	0.928	− 0.159	− 0.327	1.326	4
E_2	0.756	0.813	− 0.230	− 0.327	1.012	7
E_3	− 0.493	− 0.183	0.414	− 0.184	− 0.446	13
E_4	− 0.116	− 0.183	− 0.018	0.246	− 0.071	12
E_5	0.368	0.461	− 0.159	0.388	1.059	6
E_6	− 0.571	− 0.395	− 0.230	0.483	− 0.712	16
E_7	0.368	0.461	0.205	0.246	1.281	5
E_8	− 0.493	− 0.324	0.205	0.107	− 0.505	14
E_9	0.885	0.813	0.837	0.562	3.096	2
E_{10}	0.885	0.672	1.093	0.562	3.212	1
E_{11}	0.756	0.928	0.205	− 0.184	1.705	3
E_{12}	− 0.116	0.252	− 0.159	0.388	0.365	10
E_{13}	− 0.493	− 0.395	− 0.018	0.246	− 0.660	15
E_{14}	0.141	− 0.395	− 0.159	0.388	− 0.025	11
E_{15}	0.368	0.252	0.205	− 0.279	0.546	9
E_{16}	0.756	0.068	− 0.018	− 0.057	0.748	8

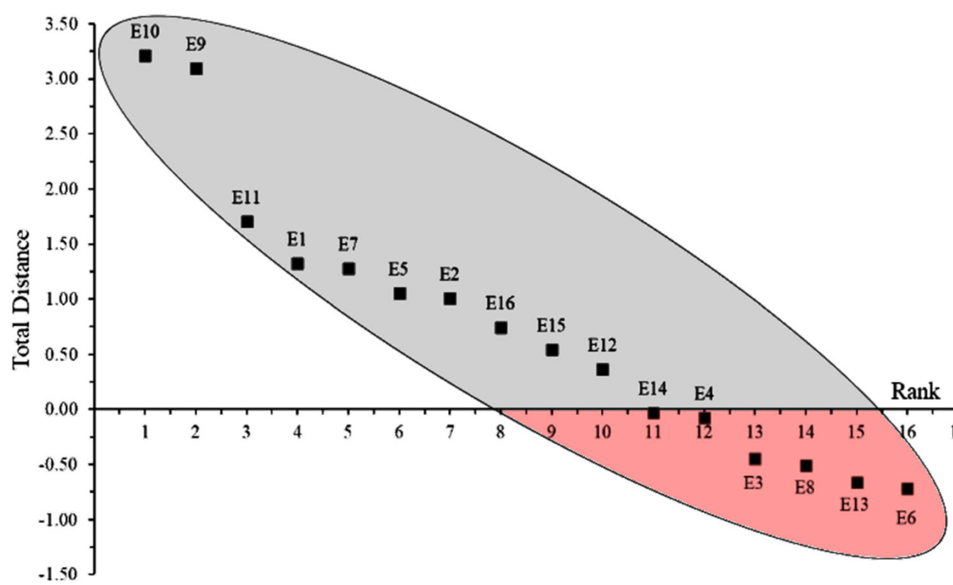

Fig. 3 Positions of the experiments in upper and lower approximation areas

Table 10 Levels of welding parameters for example 2 [28]

Welding parameter	Unit	Levels				
		− 2	− 1	0	+ 1	+ 2
Tool rotational speed (TRS)	RPM	800	1000	1200	1400	1600
Welding speed (WS)	mm/min	20	60	100	140	180
Tool offset (TO)	mm	− 2	− 1	0	1	2
Tilt angle (TA)	°	1	1.5	2	2.5	3

Table 11 Experimental data [28]

Exp. No	TRS (rpm)	WS (mm/min)	TA (°)	TO (mm)	UTS (MPa)	PE (%)	MH (HV)
E_1	1000	60	− 1	1.5	236.56	8.30	60.20
E_2	1400	60	− 1	1.5	217.00	5.70	55.30
E_3	1000	140	− 1	1.5	246.32	9.50	68.20
E_4	1400	140	− 1	1.5	236.25	8.00	60.40
E_5	1000	60	1	1.5	232.58	7.50	58.50
E_6	1400	60	1	1.5	218.60	6.70	54.60
E_7	1000	140	1	1.5	247.26	9.80	70.80
E_8	1400	140	1	1.5	233.33	7.90	58.60
E_9	1000	60	− 1	2.5	229.00	7.50	57.20
E_{10}	1400	60	− 1	2.5	214.40	6.50	54.70
E_{11}	1000	140	− 1	2.5	250.00	7.30	65.30
E_{12}	1400	140	− 1	2.5	228.00	6.90	58.50
E_{13}	1000	60	1	2.5	228.00	7.20	58.70
E_{14}	1400	60	1	2.5	215.00	6.30	55.10
E_{15}	1000	140	1	2.5	233.00	7.20	59.80
E_{16}	1400	140	1	2.5	226.90	6.80	57.60
E_{17}	1600	100	0	2	219.00	6.30	55.70
E_{18}	800	100	0	2	238.00	9.20	64.80
E_{19}	1200	180	0	2	241.00	8.90	66.50
E_{20}	1200	20	0	2	220.00	6.20	56.70
E_{21}	1200	100	2	2	220.00	6.10	55.60
E_{22}	1200	100	− 2	2	236.39	6.60	59.30
E_{23}	1200	100	0	3	215.00	6.00	54.30
E_{24}	1200	100	0	1	231.70	8.80	59.20
E_{25}	1200	100	0	2	248.00	7.50	71.50
E_{26}	1200	100	0	2	249.00	7.70	68.70
E_{27}	1200	100	0	2	254.00	7.20	69.20
E_{28}	1200	100	0	2	256.00	7.30	71.20
E_{29}	1200	100	0	2	252.00	6.90	69.60
E_{30}	1200	100	0	2	251.00	7.60	70.30

Table 12 Converting responses into SVNNs for example 2

Linguistic variable	UTS	PE	MH
Extremely good (EG)	$UTS \geq 251.38$	$PE \geq 9.34$	$MH \geq 69.59$
Very good (VG)	$246.76 \leq UTS < 251.38$	$8.88 \leq PE < 9.34$	$67.68 \leq MH < 69.59$
Good (G)	$242.14 \leq UTS < 246.76$	$8.42 \leq PE < 8.88$	$65.77 \leq MH < 67.68$
Medium good (MG)	$237.52 \leq UTS < 242.14$	$7.96 \leq PE < 8.42$	$63.86 \leq MH < 65.77$
Medium (M)	$232.90 \leq UTS < 237.52$	$7.50 \leq PE < 7.96$	$61.95 \leq MH < 63.86$
Medium bad (MB)	$228.28 \leq UTS < 232.90$	$7.04 \leq PE < 7.50$	$60.04 \leq MH < 61.95$
Bad (B)	$223.66 \leq UTS < 228.28$	$6.58 \leq PE < 7.04$	$58.13 \leq MH < 60.04$
Very bad (VB)	$219.04 \leq UTS < 223.66$	$6.12 \leq PE < 6.58$	$56.22 \leq MH < 58.13$
Extremely bad (EB)	$UTS < 219.04$	$PE < 6.12$	$MH < 56.22$

Table 13 Initial SVN – decision matrix for example 2

Exp. No	UTS			PE			MH		
	T	I	F	T	I	F	T	I	F
E_1	0.50	0.50	0.45	0.65	0.35	0.30	0.35	0.65	0.60
E_2	0.05	0.90	0.95	0.05	0.90	0.95	0.05	0.90	0.95
E_3	0.80	0.20	0.15	1.00	0.00	0.00	0.90	0.10	0.05
E_4	0.50	0.50	0.45	0.65	0.35	0.30	0.35	0.65	0.60
E_5	0.35	0.65	0.60	0.50	0.50	0.45	0.20	0.75	0.80
E_6	0.05	0.90	0.95	0.20	0.75	0.80	0.05	0.90	0.95
E_7	0.90	0.10	0.05	1.00	0.00	0.00	1.00	0.00	0.00
E_8	0.50	0.50	0.45	0.50	0.50	0.45	0.20	0.75	0.80
E_9	0.35	0.65	0.60	0.50	0.50	0.45	0.10	0.85	0.90
E_{10}	0.05	0.90	0.95	0.10	0.85	0.90	0.05	0.90	0.95
E_{11}	0.90	0.10	0.05	0.35	0.65	0.60	0.65	0.35	0.30
E_{12}	0.20	0.75	0.80	0.20	0.75	0.80	0.20	0.75	0.80
E_{13}	0.20	0.75	0.80	0.35	0.65	0.60	0.20	0.75	0.80
E_{14}	0.05	0.90	0.95	0.10	0.85	0.90	0.05	0.90	0.95
E_{15}	0.50	0.50	0.45	0.35	0.65	0.60	0.20	0.75	0.80
E_{16}	0.20	0.75	0.80	0.20	0.75	0.80	0.10	0.85	0.90
E_{17}	0.05	0.90	0.95	0.10	0.85	0.90	0.05	0.90	0.95
E_{18}	0.65	0.35	0.30	0.90	0.10	0.05	0.65	0.35	0.30
E_{19}	0.65	0.35	0.30	0.90	0.10	0.05	0.80	0.20	0.15
E_{20}	0.10	0.85	0.90	0.10	0.85	0.90	0.10	0.85	0.90
E_{21}	0.10	0.85	0.90	0.05	0.90	0.95	0.05	0.90	0.95
E_{22}	0.50	0.50	0.45	0.20	0.75	0.80	0.20	0.75	0.80
E_{23}	0.05	0.90	0.95	0.05	0.90	0.95	0.05	0.90	0.95
E_{24}	0.35	0.65	0.60	0.80	0.20	0.15	0.20	0.75	0.80
E_{25}	0.90	0.10	0.05	0.50	0.50	0.45	1.00	0.00	0.00
E_{26}	0.90	0.10	0.05	0.50	0.50	0.45	0.90	0.10	0.05
E_{27}	1.00	0.00	0.00	0.35	0.65	0.60	0.90	0.10	0.05
E_{28}	1.00	0.00	0.00	0.35	0.65	0.60	1.00	0.00	0.00
E_{29}	1.00	0.00	0.00	0.20	0.75	0.80	1.00	0.00	0.00
E_{30}	0.90	0.10	0.05	0.50	0.50	0.45	1.00	0.00	0.00

based on which a rating of very important (VI) is assigned to UTS, important (I) to PE and medium (M) to MH. Based on this information, the corresponding criteria weights, in terms of SVNNs, for UTS, PE and MH are estimated as $\langle 0.9, 0.1, 0.1\rangle$, $\langle 0.8, 0.2, 0.15\rangle$ and $\langle 0.5, 0.4, 0.45\rangle$ respectively. Using the values provided in Tables 4, 11 and 12, the initial SVN-decision matrix is now developed, as shown in Table 13. The weighted SVN-decision matrix is then derived by multiplying elements of the initial SVN-decision matrix with the corresponding criteria weights, as exhibited in Table 14. Using Eq. (13), the border approximation area matrix, given in Table 15, is calculated from the values provided in Table 14. Finally, the distance matrix is formulated based on Eq. (14). The total score for each experimental run is now derived and the runs are ranked in descending order of the total score. The corresponding distance matrix, total score and rank of each experimental run are depicted in Table 16. Based on these results, it can be noticed that experimental run 7, with parametric settings as TRS = 1000 rpm, WS = 140 mm/min, TO = 1 mm and TA = 1.5° would provide the best possible response values as UTS = 247.26 MPa, PE = 9.80% and MH = 70.80 HV. Furthermore, run 3 provides the second-best parametric combination, while runs 2 and 23 provide the worst parametric settings. Using the criterion function values, and relative positions of the conducted experimental trials in the upper and lower approximation areas, it can be unveiled that among all the 30 experiments, 19 are best performing trials superseding

Table 14 Weighted SVN-decision matrix for example 2

Exp. No	UTS			PE			MH		
	T	I	F	T	I	F	T	I	F
E_1	0.450	0.550	0.505	0.520	0.480	0.405	0.175	0.790	0.780
E_2	0.045	0.910	0.955	0.040	0.920	0.958	0.025	0.940	0.973
E_3	0.720	0.280	0.235	0.800	0.200	0.150	0.450	0.460	0.478
E_4	0.450	0.550	0.505	0.520	0.480	0.405	0.175	0.790	0.780
E_5	0.315	0.685	0.640	0.400	0.600	0.533	0.100	0.850	0.890
E_6	0.045	0.910	0.955	0.160	0.800	0.830	0.025	0.940	0.973
E_7	0.810	0.190	0.145	0.800	0.200	0.150	0.500	0.400	0.450
E_8	0.450	0.550	0.505	0.400	0.600	0.533	0.100	0.850	0.890
E_9	0.315	0.685	0.640	0.400	0.600	0.533	0.050	0.910	0.945
E_{10}	0.045	0.910	0.955	0.080	0.880	0.915	0.025	0.940	0.973
E_{11}	0.810	0.190	0.145	0.280	0.720	0.660	0.325	0.610	0.615
E_{12}	0.180	0.775	0.820	0.160	0.800	0.830	0.100	0.850	0.890
E_{13}	0.180	0.775	0.820	0.280	0.720	0.660	0.100	0.850	0.890
E_{14}	0.045	0.910	0.955	0.080	0.880	0.915	0.025	0.940	0.973
E_{15}	0.450	0.550	0.505	0.280	0.720	0.660	0.100	0.850	0.890
E_{16}	0.180	0.775	0.820	0.160	0.800	0.830	0.050	0.910	0.945
E_{17}	0.045	0.910	0.955	0.080	0.880	0.915	0.025	0.940	0.973
E_{18}	0.585	0.415	0.370	0.720	0.280	0.193	0.325	0.610	0.615
E_{19}	0.585	0.415	0.370	0.720	0.280	0.193	0.400	0.520	0.533
E_{20}	0.090	0.865	0.910	0.080	0.880	0.915	0.050	0.910	0.945
E_{21}	0.090	0.865	0.910	0.040	0.920	0.958	0.025	0.940	0.973
E_{22}	0.450	0.550	0.505	0.160	0.800	0.830	0.100	0.850	0.890
E_{23}	0.045	0.910	0.955	0.040	0.920	0.958	0.025	0.940	0.973
E_{24}	0.315	0.685	0.640	0.640	0.360	0.278	0.100	0.850	0.890
E_{25}	0.810	0.190	0.145	0.400	0.600	0.533	0.500	0.400	0.450
E_{26}	0.810	0.190	0.145	0.400	0.600	0.533	0.450	0.460	0.478
E_{27}	0.900	0.100	0.100	0.280	0.720	0.660	0.450	0.460	0.478
E_{28}	0.900	0.100	0.100	0.280	0.720	0.660	0.500	0.400	0.450
E_{29}	0.900	0.100	0.100	0.160	0.800	0.830	0.500	0.400	0.450
E_{30}	0.810	0.190	0.145	0.400	0.600	0.533	0.500	0.400	0.450

the remaining ones with respect to achieved response values. Based on a Pareto frontier developed using multi-objective biogeography-based optimization algorithm, Tamjidy et al. [28] obtained two different settings of FSW parameters in continuous solution space, i.e. TRS = 967.41 rpm, WS = 164.40 mm/min, TO = − 1.05 mm and TA = 1.97° in TOPSIS; and TRS = 1002.14 rpm, WS = 149.73 mm/min, TO = − 0.74 mm and TA = 1.92° using Shannon's entropy method. It can be noted that in both the cases, although the derived settings lie within the initial ranges of FSW parameters under consideration, they are quite difficult to set and maintain during real time welding operations. Thus, the optimal combination of FSW parameters identified using SVNS-MABAC method is more realistic as it already exists among the conducted experiments, as shown in Table 11.

During FSW process, tool rotation generates the frictional heat necessary to soften the workpiece materials for solid-state welding. At low rotational speeds, materials do not attain the proper level of plasticity, and fusion does not occur at the root and walls of the weld, leading to low tensile strength. However, increasing the tool rotational speed to a very high value can adversely impact tensile strength of the weld joint. This is because the melt material would be ejected from the butt line instead of being stirred into the weld [29]. Increasing welding speed also has a detrimental effect on tensile strength and weld quality. At high transverse/welding speeds, the welding process occurs too

Table 15 Border approximation area matrix for example 2

Criteria	UTS			PE			MH		
	T	I	F	T	I	F	T	I	F
G	0.274	0.669	0.713	0.233	0.726	0.739	0.121	0.813	0.864

Table 16 Results of the SVNS-MABAC analysis for example 2

Exp. No	UTS	PE	MH	Q_i	Rank
E_1	0.297	0.504	0.103	0.904	12
E_2	− 0.412	− 0.351	− 0.192	− 0.954	29.5
E_3	0.760	0.972	0.619	2.351	2
E_4	0.297	0.504	0.103	0.904	12
E_5	0.085	0.293	− 0.049	0.329	17
E_6	− 0.412	− 0.139	− 0.192	− 0.742	23
E_7	0.916	0.972	0.697	2.585	1
E_8	0.297	0.293	− 0.049	0.541	15
E_9	0.085	0.293	− 0.144	0.234	18
E_{10}	− 0.412	− 0.280	− 0.192	− 0.884	26
E_{11}	0.916	0.092	0.381	1.389	11
E_{12}	− 0.178	− 0.139	− 0.049	− 0.366	21
E_{13}	− 0.178	0.092	− 0.049	− 0.136	20
E_{14}	− 0.412	− 0.280	− 0.192	− 0.884	26
E_{15}	0.297	0.092	− 0.049	0.339	16
E_{16}	− 0.178	− 0.139	− 0.144	− 0.461	22
E_{17}	− 0.412	− 0.280	− 0.192	− 0.884	26
E_{18}	0.528	0.857	0.381	1.766	8
E_{19}	0.528	0.857	0.524	1.908	3
E_{20}	− 0.334	− 0.280	− 0.144	− 0.758	24
E_{21}	− 0.334	− 0.351	− 0.192	− 0.876	25
E_{22}	0.297	− 0.139	− 0.049	0.109	19
E_{23}	− 0.412	− 0.351	− 0.192	− 0.954	29.5
E_{24}	0.085	0.715	− 0.049	0.751	14
E_{25}	0.916	0.293	0.697	1.907	4
E_{26}	0.916	0.293	0.619	1.828	7
E_{27}	1.044	0.092	0.619	1.755	9
E_{28}	1.044	0.092	0.697	1.833	6
E_{29}	1.044	− 0.139	0.697	1.603	10
E_{30}	0.916	0.293	0.697	1.907	4

rapidly for enough heat to be generated to bring about sufficient softening in the material. This leads to material being removed from the pin edges instead of joining [30]. Shoulder diameter is another significant parameter influencing the weld quality. Increasing shoulder diameter would increase width of the softened material region leading to increased heat input. An increase in UTS is observed as the increased heat facilitates proper intermixing of the joining materials [31]. Higher tilt angle would lead to higher frictional heat and UTS by mixing the materials properly while avoiding welding defects, such as cavity formation, tunnelling and pinholes. However, tool rotational speed and welding speed have insignificant impacts on percentage of elongation, which is noticed to be most significantly affected by tool tilt angle. Increase in tilt angle would lead to better consolidation of material under the shoulder providing microstructures with high ductility. Therefore, there is a significant increase in percentage of elongation [32]. The hardness of the welded material would decrease with an increase in heat input. It signifies that low tool rotational speed and welding speed are detrimental to hardness as frictional heat is high [33]. Therefore, to achieve the best mechanical properties in the welded materials, the FSW process must be operated at moderate levels of the considered input parameters. Setting those parameters to very high or very low values would lead to welds with poor UTS, ductility and micro-hardness values.

5 Conclusion

In this paper, based on past experimental data, an attempt is put forward to solve parametric optimization problems of two FSW processes employing MABAC approach in single-valued neutrosophic environment. In both the examples, opinions of a single decision maker are sought while assigning criteria weights and evaluating performance of the alternative experimental trials against each response in terms of linguistic variables which are subsequently converted into corresponding SVNNs. For the first FSW process, application of SVNS-MABAC method identifies the optimal intermix of input parameters as TRS = 1200 rpm, WS = 275 mm/min, SD = 18 mm and a taper-cylindrical tool profile to provide the compromised values of UTS, YS, PE and MH. On the other hand, in the second example, the most preferred values of UTS, PE and MH can be achieved at the optimal combination of TRS = 1000 rpm, WS = 140 mm/min, TO = 1 mm and TA = 1.5°. Thus, the results derived from both the examples recommend setting all the considered welding parameters at their intermediate to slightly higher operating levels. Since these results are solely based on the past experimental data, there is no scope in this paper to validate them by conducting real time experiments. Instead of a single decision maker, opinions of multiple decision makers may be sought to derive more aggregated results in group decision making environment. Future research may include employment of MABAC in intuitionistic fuzzy, hesitant fuzzy, Pythagorean fuzzy environments etc., and application of other MCDM methods, like combined compromise solution (CoCoSo), multi-attributive ideal-real comparative analysis (MAIRCA) etc. in single-valued neutrosophic fuzzy environment for FSW processes optimization. Design and development of a decision support system to ease out the computations and automate solutions of the considered optimization problems is also highly encouraged.

Funding No external funding is required for this research study.

Declarations

Conflict of interest The authors declare no competing interests.

References

1. Sun, Y., Gong, W., Feng, J., Lu, G., Zhu, R., Li, Y.: A review of the friction stir welding of dissimilar materials between aluminium alloys and copper. Metals **12**, 675 (2022)
2. Christy, J.V., Mourad, A.H.I., Sherif, M.M., Shivamurthy, B.: Review of recent trends in friction stir welding process of aluminium alloys and aluminium metal matrix composites. Trans. Nonferrous Met. Soc. China **31**, 3281–3309 (2021)
3. Rudrapati, R.: Effects of welding process conditions on friction stir welding of polymer composites: A review. Composites Part C **8**, 100269 (2022)
4. Cam, G., Mistikoglu, S.: Recent developments in friction stir welding of Al-alloys. J. Mater. Eng. Perform. **23**, 1936–1953 (2014)
5. Ma, Z.Y., Feng, A.H., Chen, D.L., Shen, J.: Recent advances in friction stir welding/processing of aluminium alloys: Microstructural evolution and mechanical properties. Crit. Rev. Solid State Mater. Sci. **43**, 269–333 (2018)
6. Mohan, D.G., Wu, C.: A review on friction stir welding of steels. Chin. J. Mech. Eng. **34**, 1–29 (2021)
7. Sharma, S., Handa, A., Singh, S.: Influencing geometrical parameters of tools in friction stirring technology: A short review. J. Mech. Eng. **71**, 257–290 (2021)
8. Janeczek, A., Tomkow, J., Fydrych, D.: The Influence of tool shape and process parameters on mechanical properties of AW-3004 aluminium alloy friction stir welded joints. Materials **14**, 3244 (2021)
9. Shehabeldeen, T.A., Abd Elaziz, M., Elsheikh, A.H., Zhou, J.: Modeling of friction stir welding process using adaptive neuro-fuzzy inference system integrated with Harris Hawks optimizer. J. Market. Res. **8**, 5882–5892 (2019)
10. Nguyen, T.T., Nguyen, C.T., Van, A.L.: Sustainability-based optimization of dissimilar friction stir welding parameters in terms of energy saving, product quality, and cost-effectiveness. Neural Comput. Appl. (2022). https://doi.org/10.1007/s00521-022-07898-8
11. Van, A.L., Nguyen, T.T.: Optimization of friction stir welding operation using optimal Taguchi-based ANFIS and genetic algorithm. J. Mech. Eng. **68**, 424–438 (2022)
12. Babajanzade Roshan, S., Behboodi Jooibari, M., Teimouri, R., Asgharzadeh-Ahmadi, G., Falahati-Naghibi, M., Sohrabpoor, H.: Optimization of friction stir welding process of AA7075 aluminium alloy to achieve desirable mechanical properties using ANFIS and simulated annealing algorithm. Int. J. Adv. Manuf. Technol. **69**, 1803–1818 (2013)
13. Vijayan, D., Seshagiri Rao, V.: Parametric optimization of friction stir welding process of age hardenable aluminium alloys—ANFIS modelling. J. Cent. South Univ. **23**, 1847–1857 (2016)
14. Deepandurai, K., Parameshwaran, R.: Multiresponse optimization of FSW parameters for cast AA7075/SiCp composite. Mater. Manuf. Processes **31**, 1333–1341 (2016)
15. Parida, B., Pal, S.: Fuzzy assisted grey Taguchi approach for optimisation of multiple weld quality properties in friction stir welding process. Sci. Technol. Weld. Joining **20**, 35–41 (2015)
16. Sahu, P., Kumari, K., Pal, S., Pal, S.K.: Hybrid fuzzy-grey-Taguchi based multi weld quality optimization of Al/Cu dissimilar friction stir welded joints. Adv. Manuf. **4**, 237–247 (2016)
17. Chauhan, A., Kumar, S.: An overview of optimization techniques used for friction stir welding process parameters. Res. J. Eng.Technol. **9**, 21–26 (2018)
18. Singh MK, Porwal RK, Mishra S (2020) Optimization-related studies on the operational parameters of friction stir welding: An overview. In: Singh I, Bajpai P, Panwar K (eds) Trends in Manufacturing Processes. Lecture Notes on Multidisciplinary Industrial Engineering. Springer, Singapore https://doi.org/10.1007/978-981-32-9099-0_1

19. Zadeh, L.A.: Fuzzy sets. Inf. Control **8**, 338–353 (1965)
20. Atanassov, K.T.: Intutionistic fuzzy sets. Fuzzy Sets Syst. **20**, 87–96 (1986)
21. Smarandache F (1999) A unifying field in logics: Neutrosophic logic. In: Philosophy, American Research Press 1–141
22. Biswas, P., Pramanik, S., Giri, B.C.: Entropy based grey relational analysis for multi-attribute decision making under single valued neutrosophic assessments. Neutrosophic Sets Syst. **2**, 102–110 (2014)
23. Wang, H., Smarandache, F., Zhang, Y., Sunderraman, R.: Single valued neutrosophic sets. Multispace Multistruct. **4**, 410–413 (2010)
24. Pamučar, D., Ćirović, G.: The selection of transport and handling resources in logistics centers using multi-attributive border approximation area comparison (MABAC). Expert Syst. Appl. **42**, 3016–3028 (2015)
25. Peng, X., Dai, J.: Approaches to single-valued neutrosophic MADM based on MABAC, TOPSIS and new similarity measure with score function. Neural Comput. Appl. **29**, 939–954 (2018)
26. Jain, N., Kumar, R.: Multi-response optimization of process parameters in friction stir welded aluminium 6061–T6 alloy using Taguchi grey relational analysis. World J. Eng. **19**, 707–716 (2022)
27. Biswas, P., Pramanik, S., Giri, B.C.: TOPSIS method for multi-attribute decision-making under single-valued neutrosophic environment. Neural Comput. Appl. **27**, 727–737 (2016)
28. Tamjidy, M., Baharudin, B.H.T., Paslar, S., Matori, K.A., Sulaiman, S., Fadaeifard, F.: Multi-objective optimization of friction stir welding process parameters of AA6061-T6 and AA7075-T6 using a biogeography-based optimization algorithm. Materials **10**, 533 (2017)
29. Saeedy, S., Givi, M.B.: Investigation of the effects of critical process parameters of friction stir welding of polyethylene. Proc. Inst. Mech. Eng. Part B J. Eng. Manuf. **225**, 1305–1310 (2011)
30. Aydin, M.: Effects of welding parameters and pre-heating on the friction stir welding of UHMW-polyethylene. Polym. Plast. Technol. Eng. **39**, 595–601 (2010)
31. Fuse, K., Badheka, V.: Effect of shoulder diameter on bobbin tool friction stir welding of AA 6061–T6 alloy. Mater. Today Proc. **42**, 810–815 (2021)
32. Kadaganchi, R., Gankidi, M.R., Gokhale, H.: Optimization of process parameters of aluminium alloy AA 2014–T6 friction stir welds by response surface methodology. Def. Technol. **11**, 209–219 (2015)
33. Rajamanickam, N., Balusamy, V.: Effects of process parameters on mechanical properties of friction stir welds using design of experiments. Indian J. Eng. Mater. Sci. **15**, 293–299 (2008)

Publisher's Note Springer Nature remains neutral with regard to jurisdictional claims in published maps and institutional affiliations.

Springer Nature or its licensor (e.g. a society or other partner) holds exclusive rights to this article under a publishing agreement with the author(s) or other rightsholder(s); author self-archiving of the accepted manuscript version of this article is solely governed by the terms of such publishing agreement and applicable law.